Radiocarbon, Vol 66, Nr 6, 2024, p 1940–1957 DOI:10.1017/RDC.2023.63
Selected Papers from the 24th Radiocarbon and 10th Radiocarbon & Archaeology International Conferences, Zurich, Switzerland, 11–16 Sept. 2022.

ALTERNATIVE RADIOCARBON AGE-DEPTH MODEL FROM LAKE BAIKAL SEDIMENT: IMPLICATION FOR PAST HYDROLOGICAL CHANGES FOR LAST GLACIAL TO THE HOLOCENE

Fumiko Watanabe Nara[1,2,3]* • Takahiro Watanabe[4] • Bryan C Lougheed[5] • Stephen Obrochta[6]

[1]Graduate School of Environmental Science, Nagoya University, Furo-cho, Chikusa, Nagoya, 464-8601, Japan
[2]Low Level Radioactivity Laboratory, Institute of Nature and Environmental Technology, Kanazawa University, O 24, Wake, Nomi, Ishikawa 923-1224, Japan
[3]Faculty of Liberal Arts and Science, Chukyo University, 101-2 Yagoto Honmachi, Showa, Nagoya, 466-8666, Japan
[4]Tono Geoscience Center, Japan Atomic Energy Agency, Joringi, Izumi-cho, Toki, 509-5102, Japan
[5]Department of Earth Sciences, Uppsala University, Uppsala, Sweden
[6]Graduate School of International Resource Science, Akita University, Akita, Japan

ABSTRACT. We present an alternative radiocarbon (^{14}C) age-depth model using IntCal20 to calibrate new accelerator mass spectrometry (AMS) data applied to a Lake Baikal sediment core (VER99G12) in southern Siberia. ^{14}C dating showed that the core extends to 31 ka. To take into account uncertainties in ^{14}C age and sedimentation depth in the core, a new age-depth modeling routine, *undatable*, was used in this study. *Undatable* revealed that significant changes in sedimentation rate correspond to global climate events, either warm or cold, which periods are likely close to the timing of the occurrence of the Meltwater pulses (MWP) at 19 and 14 ka, and the Last glacial Maximum (LGM) at 21–20 ka. Since the Selenga River accounts for 50% of the total river inflow to Lake Baikal, we interpret that these changes in sedimentation rate could be signals of significant changes in Selenga River discharge to the lake, which is expected to be affected by global climate change. Based on pollen analysis, it is highly probable that the sudden influx of the Selenga River to Lake Baikal, particularly at 19 ka, was due to the thawing of permafrost water through the Selenga River, which had developed in the region. Total organic carbon content and mean grain size increases concurrent with sedimentation rate, suggesting river inflow increased available nutrients for biological activity. Our results indicate that hydrological changes corresponding to MWP events can be observed in continental areas of the Northern Hemisphere.

KEYWORDS: melt water pulse, sedimentation rates, Selenga River, *Undatable* age modeling.

INTRODUCTION

Lake Baikal, which is located in the south Siberian region (Figure 1), is the world's oldest (at least 30Ma) and deepest (1648 m) lake with the largest water volume (23,000 km^3), which represents ~20% of the total unfrozen freshwater on the earth. Because long, continuous past environmental records (Kashiwaya et al. 2001) in the south Siberian region are preserved at its basin, numerous studies using lake sediment cores from Lake Baikal have been carried out to understand the past climate and environmental histories in the south Siberian region (Colman et al. 1995; Horiuchi et al. 2000; Kashiwaya et al. 2001; Karabanov et al. 2004; Prokopenko et al. 2006; Shichi et al. 2007, 2013; Tani et al. 2009). The inseparable linkage to the global climate changes and orbital climate forcing, such as glacial and inter glacial climate cycles and the Milankovitch cycles, respectively, have been revealed (Colman et al. 1995; Kashiwaya et al. 2001; Ochiai and Kashiwaya 2003, 2005; Prokopenko et al. 2006). Therefore, Lake Baikal has been regarded as an iconic site in the Siberian region for scientific study (Arzhannikov et al. 2018).

To reconstruct the paleoenvironmental changes using a lacustrine sediment core, the establishments of a precise age model is essential. Approaches for Lake Baikal age-depth models, especially for the late Quaternary period, are based on radioactive nuclides, such as ^{10}Be, ^{14}C, ^{137}Cs, ^{210}Pb, ^{237}Am, and U/Th (Horiuchi et al. 2003; Chebykin et al. 2007; Watanabe

*Corresponding author. Email: narafumi@nagoya-u.jp

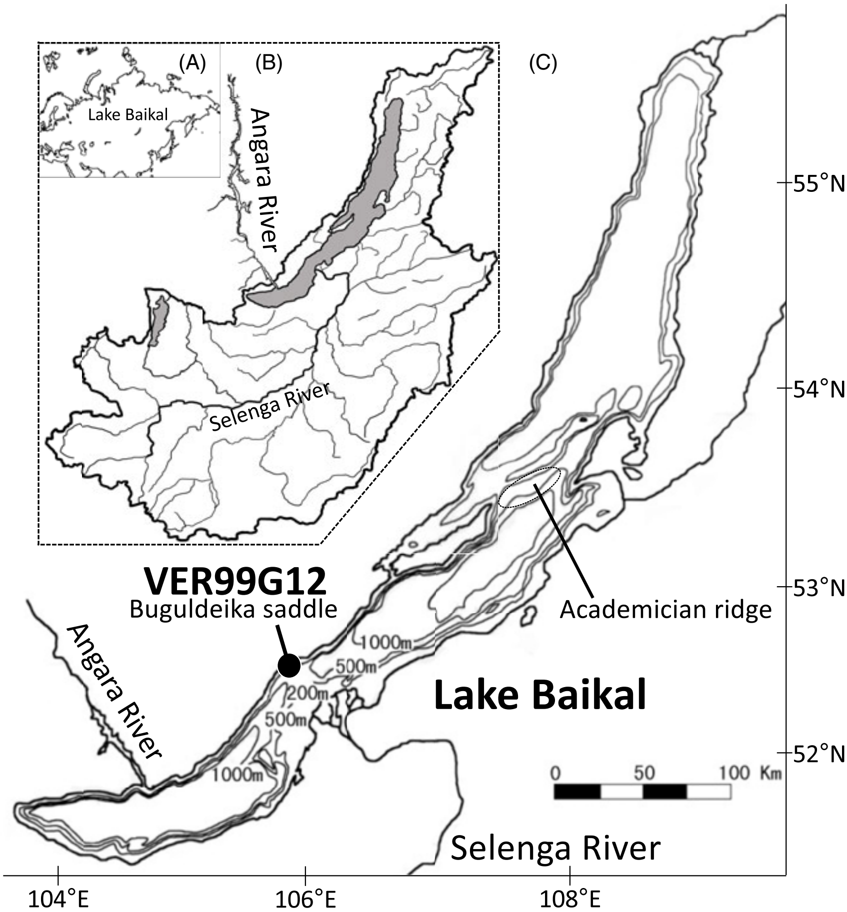

Figure 1 Map showing (A) the Eurasian continent, (B) Lake Baikal and its watershed and (C) Lake Baikal and the sampling site of the core VER99G12. The maps of Lake Baikal and its watershed were created with reference to Kuzumin et al. (2000). Lake Baikal is located at middle latitudes of the Eurasian continent (51.5–55.8°N, 103.7–109.0°E) and stores the largest volume of freshwater on Earth.

et al. 2009a; Nara et al. 2010; Swann et al. 2018), paleomagnetic records (Antipin et al. 2001; Demory et al. 2005), and orbital tuning (Ochiai and Kashiwaya 2005). Among of them, radiocarbon (^{14}C) age models have been widely applied to determine the deposition age of the Lake Baikal sediment during the last glacial to the Holocene (Colman et al. 1996; Horiuchi et al. 2000; Prokopenko et al. 2001; Soma et al. 2006; Nara et al. 2014). Lake Baikal sediments lack biogenic and authigenic carbonate for ^{14}C measurement, as well as the plant macrofossils, leading to ^{14}C dating approaches based on using total organic carbon (TOC).

The first reported ^{14}C age-depth model of the Lake Baikal sediment cores (Colman et al. 1996) showed the ^{14}C age-depth profiles measured by accelerator mass spectrometer (AMS) at two iconic sampling sites from Academician Ridge and Buguldeika Saddle (Figure 1C). These sites are topographically high and divided the basins into the Northern and the Central Basins for Academician Ridge, and into the Central and Southern Basin for Buguldeika Saddle

https://doi.org/10.1017/RDC.2023.63 Published online by Cambridge University Press

(Figure 1C). Colman et al. (1996) concluded that the reservoir effect is limited to about 1000 ± 500 ^{14}C yr for these sites, because of the most of organic carbon in Lake Baikal is autochthonous. The ^{14}C age-depth profiles at these sites described the constant linear sedimentation rates of about 4 cm/kyr and 14 cm/kyr from Academician Ridge and Buguldeika Saddle, respectively (Colman et al. 1996). Further intensive study with high temporal resolution ^{14}C analysis from three Lake Baikal sediment cores at Academician Ridge was conducted by Watanabe et al. (2009a) to develop a precise ^{14}C age model of TOC. Their work revealed the known ^{14}C activity plateau at the Younger Dryas (YD)/Preboreal (PB) boundary, which resulted from the changes in the atmospheric radiocarbon concentration during the cooling period. This ^{14}C plateau allowed for the application of radiocarbon wiggle-match dating, providing an estimation of the reservoir effect of ~2100 ^{14}C yr for the site at Academician Ridge. Since ^{14}C ages of TOC in the lacustrine sediments can be influenced by the lake reservoir effect, the hard-water effect, and the effect of the terrestrial organic matter (Watanabe et al. 2009a), it is very important to consider their effects on the ^{14}C ages of TOC in order to obtain and accurate ^{14}C age-depth model from the Academician Ridge sediment core.

Nara et al. (2010) previously showed a calibrated ^{14}C age-depth profile measured from TOC and pollen grains from core VER99G12 which was retrieved from Buguldeika saddle and spanned for the past 33 cal kyr BP (Figure 1C). Although changes in the organic carbon source at the corresponding periods would also alter the ^{14}C age, the ^{14}C ages of pollen and total lipids were not significantly different from those of TOC in the core VER99G12 (Table 1; Watanabe et al. 2009a; Nara et al. 2010), suggesting that TOC is a suitable material for ^{14}C dating in this case. Furthermore, it is reported that TOC and total nitrogen were significantly positively correlated with zero intercept throughout the core, meaning that TOC was negligibly contributed by allochthonous sources such as lignin and cellulose (Nara et al. 2014). These results indicate the significant reservoir effect on TOC in the core VER99G12 would be negligible.

In this study, we present additional ^{14}C of TOC results (20 samples) from the VER99G12 to establish the alternative ^{14}C age model for the core VER99G12 based on IntCal20 (Reimer et al. 2020), especially for the climate transition period from the Last Glacial Maximum to the onset of the Holocene (20.8–11.7 ka; Ishiwa et al. 2016), using *Undatable* age model approach. The routine *Undatable* uses a deterministic approach to fold the sampling distance into total uncertainty and is designed to efficiently model age-depth relationships using an iterative procedure to explore multiple model settings. *Undatable* has previously been successfully to establishing accurate age-depth models for marine and lacustrine sedimentary achieves (Obrochta et al. 2018; Lougheed and Obrochta 2019; Waelbroeck et al. 2019). Recent refinements in the calibrations curve (Reimer et al. 2020) that have been made available since the last publication of the age model of the VER99G12 (Nara et al. 2010) reveal that the sedimentation processes on the Buguldeika saddle in Lake Baikal have been strongly influenced by the global climate events, resulting in the rapid changes in the sedimentation rate of the core.

STUDY AREA AND SEDIMENT SAMPLES

The location of Lake Baikal in Eurasian continent, the Lake Baikal watershed and the sampling site of the core VER99G12 are shown in a map in Figure 1. Owing to this large watershed, more than 80% of the water entering the lake comes from rivers (Osipov and Khlystov 2010); and less than 2% is contributed by precipitation on the lake surface. The

https://doi.org/10.1017/RDC.2023.63 Published online by Cambridge University Press

Table 1 Conventional ^{14}C ages and calibrated ages of TOC, total lipids, and pollen fractions from the core VER99G12 from Lake Baikal.

Core depth (cm)	Material	Conventional ^{14}C age ± measurement error (^{14}C yr BP)	Calibrated age Highest posterior density 95.45% interval(s) (cal yr BP)	Calibrated age median (cal yr BP)	Lab code	References
3 – 4	TOC	1793 ± 28	1741–1688 (40.1%), 1674–1604 (55.4%)	1661	NUTA2-8898	Watanabe et al. 2007
3 – 4	Total lipids	1805 ± 35	1820–1806 (2.3%), 1796–1689 (52.5%), 1674–1606 (40.7%)	1700	NUTA2-10756	Watanabe et al. 2009b
12 – 13	TOC	3219 ± 30	3480–3473 (3.2%), 3470–3374 (92.4%)	3424	NUTA2-8899	Watanabe et al. 2007
12 – 13	Total lipids	3105 ± 29	3385–3233 (95.5%)	3316	NUTA2-10540	Watanabe et al. 2009b
54 – 55	TOC	4792 ± 32	5588–5473 (95.5%)	5522	NUTA2-8900	Watanabe et al. 2007
54 – 55	Total lipids	4644 ± 28	5464–5371 (74%), 5362–5342 (6.4%), 5334–5312 (15.2%)	5407	NUTA2-10543	Watanabe et al. 2009b
104 – 105	TOC	7673 ± 37	8541–8393 (95.7%)	8456	NUTA2-8901	Watanabe et al. 2007
104 – 105	Total lipids	7522 ± 32	8401–8301 (78.1%), 8261–8206 (17.4%)	8349	NUTA2-10544	Watanabe et al. 2009b
121 – 123	Pollen fraction	8684 ± 108	10130–10061 (5%), 10042–10021 (1.2%), 10014–9987 (1.6%), 9963–9488 (87.6%)	9705	NUTA2-11629	Nara et al. 2010
122 – 123	TOC	8545 ± 27	9543–9488 (95.5%)	9527	NUTA2-11632	Watanabe et al. 2009b
124 – 126	Pollen fraction	8722 ± 115	10153–9982 (15.3%), 9968–9533 (80.2%)	9760	NUTA2-11630	Nara et al. 2010

(Continued)

https://doi.org/10.1017/RDC.2023.63 Published online by Cambridge University Press

Table 1 (*Continued*)

Core depth (cm)	Material	Conventional ^{14}C age ± measurement error (^{14}C yr BP)	Calibrated age Highest posterior density 95.45% interval(s) (cal yr BP)	Calibrated age median (cal yr BP)	Lab code	References
129 – 131	Pollen fraction	8814 ± 49	10154–9981 (24.4%), 9969–9668 (71%), 9635–9635 (0%)	9855	NUTA2-11631	Nara et al. 2010
130 – 131	TOC	9131 ± 29	10403–10396 (1%), 10381–10227 (94.6%)	10269	NUTA2-11633	Watanabe et al. 2009b
139 – 140	TOC	9688 ± 36	11209–11070 (75.5%), 10949–10872 (17.5%), 10842–10813 (2.5%)	11129	NUTA2-13990	Nara et al. 2010
150 – 151	TOC	8975 ± 36	10233–10117 (66.9%), 10065–10007 (12.9%), 9992–9956 (12.5%), 9943–9917 (3.2%)	10166	NUTA2-13991	Nara et al. 2010
154 – 155	TOC	9882 ± 45	11460–11455 (0.3%), 11401–11201 (95.2%)	11282	NUTA2-13254	Nara et al. 2010
154 – 155	Total lipids	9356 ± 43	10698–10489 (90.1%), 10461–10429 (5.4%)	10570	NUTA2-10747	Watanabe et al. 2009b
156 – 157	TOC	9210 ± 36	10495–10455 (14.1%), 10440–10250 (81.4%)	10363	NUTA2-13992	Nara et al. 2010
159 – 160	TOC	9453 ± 39	11060–11042 (1.7%), 10998–10972 (3.8%), 10780–10574 (90%)	10684	NUTA2-10711	Watanabe et al. 2009b
162 – 163	TOC	9479 ± 36	11066–11029 (6.6%), 11006–10963 (10.3%), 10865–10855 (0.8%), 10797–10642 (66.8%), 10634–10582 (11%)	10723	NUTA2-13993	Nara et al. 2010

https://doi.org/10.1017/RDC.2023.63 Published online by Cambridge University Press

Table 1 (*Continued*)

Core depth (cm)	Material	Conventional ^{14}C age ± measurement error (^{14}C yr BP)	Calibrated age Highest posterior density 95.45% interval(s) (cal yr BP)	Calibrated age median (cal yr BP)	Lab code	References
164 – 165	TOC	10164 ± 50	11971–11609 (93.2%), 11528–11504 (1.5%), 11424–11409 (0.7%)	11808	NUTA2-9597	Watanabe et al. 2007
164 – 165	Total lipids	10971 ± 45	13060–13025 (5.5%), 13003–12762 (90.1%)	12877	NUTA2-10748	Watanabe et al. 2009b
167 – 168	TOC	11105 ± 49	13112–12897 (95.5%)	13019	NUTA2-10723	Watanabe et al. 2009b
174 – 175	TOC	11834 ± 53	13793–13590 (92.3%), 13542–13523 (3.3%)	13685	NUTA2-9604	Watanabe et al. 2007
189 – 190	TOC	12571 ± 41	15135–14817 (85.9%), 14704–14584 (9.6%)	14965	NUTA2-13985	Nara et al. 2010
198 – 199	TOC	11928 ± 42	14015–13923 (23.6%), 13872–13736 (55.3%), 13712–13647 (11.3%), 13635–13608 (5.2%)	13792	NUTA2-13986	Nara et al. 2010
200 – 201	TOC	11785 ± 49	13767–13577 (80.3%), 13554–13508 (15.2%)	13651	NUTA2-13255	Nara et al. 2010
202 – 203	TOC	12433 ± 65	14960–14241 (95.5%)	14581	NUTA2-13257	Nara et al. 2010
204 – 205	TOC	12289 ± 41	14804–14710 (9.9%), 14430–14429 (0.1%), 14424–14390 (1.3%), 14358–14074 (84.2%)	14218	NUTA2-13989	Nara et al. 2010
205 – 206	TOC	11234 ± 138	13408–13375 (1.7%), 13365–12838 (93.8%)	13139	JAT-12144	This study

(*Continued*)

https://doi.org/10.1017/RDC.2023.63 Published online by Cambridge University Press

Table 1 (*Continued*)

Core depth (cm)	Material	Conventional ^{14}C age ± measurement error (^{14}C yr BP)	Calibrated age Highest posterior density 95.45% interval(s) (cal yr BP)	Calibrated age median (cal yr BP)	Lab code	References
207 – 208	TOC	11731 ± 119	13979–13957 (0.7%), 13805–13322 (94.7%)	13596	JAT-12145	This study
209 – 210	TOC	12022 ± 134	14291–14263 (0.7%), 14254–13590 (94.2%), 13543–13522 (0.6%)	13912	JAT-12146	This study
211 – 212	TOC	12518 ± 122	15195–14204 (95.5%)	14715	JAT-12147	This study
213 – 214	TOC	12773 ± 120	15649–14873 (95.5%)	15246	JAT-12148	This study
214 – 215	TOC	12705 ± 54	15304–14979 (95.5%)	15150	NUTA2-9602	Watanabe et al. 2007
214 – 215	Total lipids	13167 ± 50	15978–15638 (95.5%)	15797	NUTA2-10750	Watanabe et al. 2009b
215 – 216	TOC	13841 ± 121	17093–16381 (95.5%)	16790	JAT-12149	This study
217 – 218	TOC	13575 ± 118	16812–16019 (95.5%)	16395	JAT-12150	This study
218 – 219	TOC	13810 ± 47	16969–16570 (95.5%)	16767	NUTA2-10716	Watanabe et al. 2009b
222 – 223	TOC	14690 ± 49	18189–17847 (95.5%)	18024	NUTA2-10715	Watanabe et al. 2009b
230 – 231	TOC	15154 ± 52	18647–18273 (95.5%)	18481	NUTA2-10712	Watanabe et al. 2009b
240 – 241	TOC	15714 ± 56	19108–18861 (95.5%)	18969	NUTA2-8905	Watanabe et al. 2007
240 – 241	Total lipids	14886 ± 53	18284–18085 (95.5%)	18211	NUTA2-10754	Watanabe et al. 2009b
250 – 251	TOC	15964 ± 68	19477–19090 (95.5%)	19275	NUTA2-9601	Watanabe et al. 2007

https://doi.org/10.1017/RDC.2023.63 Published online by Cambridge University Press

Table 1 (*Continued*)

Core depth (cm)	Material	Conventional ^{14}C age ± measurement error (^{14}C yr BP)	Calibrated age Highest posterior density 95.45% interval(s) (cal yr BP)	Calibrated age median (cal yr BP)	Lab code	References
253 – 254	TOC	15627 ± 127	19178–18689 (95.5%)	18914	JAT-12151	This study
259 – 260	TOC	15410 ± 121	18924–18590 (73.2%), 18505–18297 (22.2%)	18717	JAT-12152	This study
261 – 262	TOC	15324 ± 125	18839–18552 (52.5%), 18540–18284 (43%)	18607	JAT-12153	This study
263 – 264	TOC	15744 ± 121	19347–18807 (95.5%)	19022	JAT-12154	This study
265 – 266	TOC	16139 ± 69	19615–19219 (95.5%)	19480	NUTA2-9600	Watanabe et al. 2007
266 – 267	TOC	15923 ± 123	19509–18939 (95.5%)	19227	JAT-12155	This study
267 – 268	TOC	17430 ± 71	21325–20862 (95.5%)	21022	NUTA2-13258	Watanabe et al. 2007
268 – 269	TOC	14662 ± 117	18221–17515 (95.5%)	17954	JAT-12156	This study
269 – 270	TOC	16464 ± 128	20222–19552 (95.5%)	19871	JAT-12157	This study
272 – 273	TOC	17551 ± 58	21394–20976 (95.5%)	21188	NUTA2-10718	Watanabe et al. 2009b
274 – 275	TOC	16671 ± 124	20484–19840 (95.5%)	20149	JAT-12159	This study
277 – 278	TOC	17649 ± 72	21715–21527 (12.2%), 21519–21025 (83.2%)	21328	NUTA2-10724	Watanabe et al. 2009b
277 – 278	TOC	17011 ± 126	20867–20272 (95.5%)	20563	JAT-12160	This study
278 – 279	TOC	17154 ± 126	20970–20436 (95.5%)	20704	JAT-12161	This study
281 – 282	TOC	16619 ± 125	20432–19803 (91.7%), 19723–19628 (3.8%)	20083	JAT-12161	This study
284 – 285	TOC	18173 ± 73	22314–21964 (95.5%)	22134	NUTA2-10719	Watanabe et al. 2009b

(*Continued*)

https://doi.org/10.1017/RDC.2023.63 Published online by Cambridge University Press

Table 1 (*Continued*)

Core depth (cm)	Material	Conventional ^{14}C age ± measurement error (^{14}C yr BP)	Calibrated age Highest posterior density 95.45% interval(s) (cal yr BP)	Calibrated age median (cal yr BP)	Lab code	References
285 – 286	TOC	17747 ± 127	21956–21062 (95.5%)	21548	JAT-12162	This study
287 – 288	TOC	17436 ± 127	21440–20722 (95.5%)	21070	JAT-12163	This study
303 – 304	TOC	19543 ± 71	23788–23304 (95.5%)	23517	NUTA2-8906	Watanabe et al. 2007
303 – 304	Total lipids	18825 ± 66	22954–22524 (95.5%)	22749	NUTA2-10755	Watanabe et al. 2009b
400 – 401	TOC	23654 ± 91	27943–27659 (95.5%)	27788	NUTA2-8907	Watanabe et al. 2007
460 – 461	TOC	27162 ± 130	31506–31054 (95.5%)	31195	NUTA2-10723	Watanabe et al. 2009b

sediment core sample in this study (VER99G12; 52º31'36"N, 106º09'08"E) was extracted from the Buguldeika saddle in Lake Baikal, which is geomorphologically separated from the central and southern basins. The sediment core sample was mainly formed by deposition materials from Selenga River (Kuzumin et al. 2000), which provides the largest inflow to Lake Baikal (ca. 50% of the total river input) (Osipov and Khlystov 2010). Therefore, the VER99G12 core records the climate and environmental changes not only in the Lake Baikal water column but also in its watershed, including the semi-arid region in Mongolia (Figure 1B). A number of paleoenvironmental studies using the core VER99G12 have been carried out (Soma et al. 2006; Nara et al. 2010; Shichi et al. 2013; Nara et al. 2014; Katsuta et al. 2018). These studies confirmed that the core VER99G12 is an excellent archive for understanding biological and hydrological changes in the south Siberian region caused by global climate changes, such as the last glacial to the post glacial change.

MATERIAL AND METHODS

Radiocarbon Measurements

The bulk sediment samples, retrieved from the core VER99G12 (Table 1) for the ^{14}C measurements, were aliquoted into individual glass vials and stored in a freezer at −20ºC until the time of analysis. Samples were treated with 1.2 N-HCl to remove any carbonates. All the treated ^{14}C samples were combusted at 850ºC for 6 hr in evacuated tubes with CuO and Ag wire. The resulting CO_2 was collected and purified in a vacuum line and reduced to graphite using an iron catalyst and hydrogen at 650ºC for 6 hr. The ^{14}C measurements were performed by an accelerator mass spectrometer (JAEA-AMS-TONO-5MV; 15SDH-2, National Electrostatics Corporation) in the TONO Geoscience Center, Japan Atomic Energy Agency. Calibration to calendar ages for the ^{14}C ages were performed using MatCal (Lougheed and Obrochta 2016) and the IntCal20 calibration curve (Reimer et al. 2020). Although the ^{14}C age-depth model of the VER99G12 core has been previously inferred from the previous IntCal datasets (Nara et al. 2010; Katsuta et al. 2018), we recalibrated the ^{14}C age of the core based on the updated IntCal20 dataset (Reimer et al. 2020; see Table 1).

Age Model Construction Using *Undatable*

Age modeling using *Undatable* was established following the previously reported studies in Lougheed and Obrochta (2019) and Obrochta et al. (2018). *Undatable* was developed out of a need to handle datasets with both high age-depth scatter and a disturbed depth scale by being less optimistic regarding uncertainty than the typical Bayesian models. The initial version was developed to model age in highly expanded cores from the Baltic Sea (Obrochta et al. 2017), was further modified to model coral growth rates (Webster et al. 2018), and further refined by Obrochta et al. (2018). Lougheed and Obrochta (2019) then substantially optimized the routine to be currently the most efficient model (to our knowledge) available for determining age in geological archives. Model parameters were 10^5 simulations, 0.1 sedimentation rate uncertainty factor, and 30% bootstrapping, excluding intervals with dates in stratigraphic order in the upper ~1 m, at ~170 cm and below ~300 cm. Although the reservoir effect by older carbon on total organic carbon date for the Buguldeika saddle in Lake Baikal could be significantly small (Nara et al. 2014), we used 380 ^{14}C yr for the reservoir effect in *Undatable* to establish the age model because of its water residence time (Shimaraev et al. 1993).

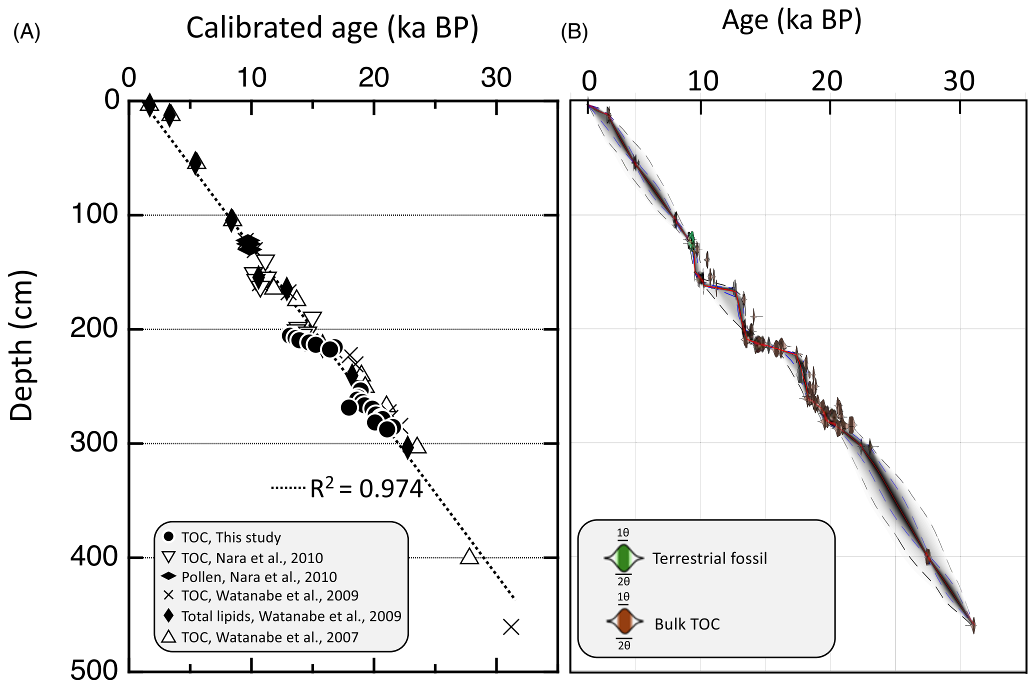

Figure 2 Calibrated age model for the core VER99G12. (A) *Undatable* age model of core VER99G12, (B)Vertical distributions of calibrated ages for core VER99G12, and (C) limited to a sediment depth of 100–300 m of calibrated ages for core VER99G12. The dashed line in Figure 2B is a regression line for the calibrated age through the core. Correlation coefficient between the calibrated age and the depth through the core was calculated in 0.974. Dark and light shading in calendar age probability density functions (PDFs), indicates the calibrated 68.2% and 95.4% age ranges, respectively. The modeled median age and 95.4% range are indicated by the red solid and black dashed lines, receptively. The shaded density cloud reflects the 1 to 99th percentile range.

RESULTS

All ^{14}C data of the core VER99G12 are summarized in Table 1. The depth profiles of combined all calibrated age data of the core VER99G12 alongside *Undatable* were shown in Figure 2. The ^{14}C age of the bottom layer (461–460 cm) was determined as ~31,000 cal years BP (Table 1), which spans the marine isotope stage 3. The calibrated age depth profiles show the linear sedimentation rates (ca. 13.3 cm/kyr) with the high correlation coefficient through the core ($R^2 = 0.974$) through the core (Figure 2B). Nevertheless, the high-time-resolution ^{14}C dating from 300 to 100 cm depth in the core VER99G12 (Figure 2C) studied here showed notable fluctuations at the layer from 260 to 120 cm depth.

The set of assumptions built in to an age-depth model affects the resulting estimate of uncertainty. While Bacon (Blaauw and Christen 2011) treats age-depth determinations that are not in stratigraphic order as outliers that should not contribute to uncertainty, Undatable includes information from such determinations by increasing age-depth model uncertainty, particularly if bootstrapping (i.e., the number of dates to randomly exclude from a single Monte Carlo iteration), is relatively high. Reworking and bioturbation in marine and lacustrine settings mixes older and younger sediment, which, combined with sampling resolution, can lead to apparent age-depth reversals and increasing uncertainty. Undatable also

https://doi.org/10.1017/RDC.2023.63 Published online by Cambridge University Press

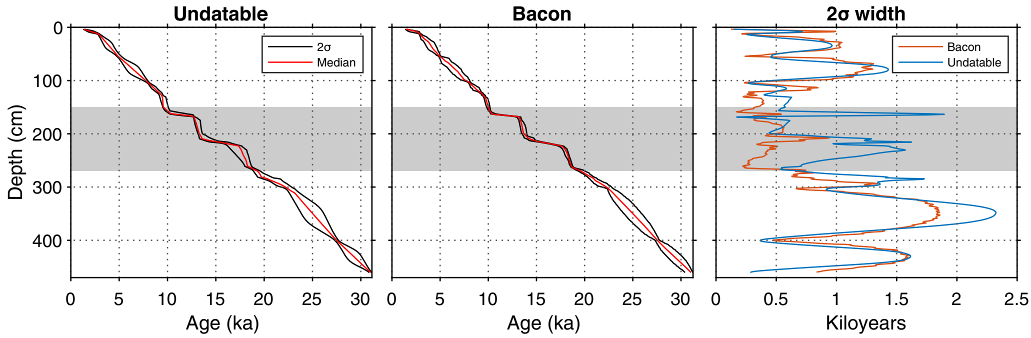

Figure 3 VER99G12 age models produced with Undatable (left panel; using parameters described in the Methods) and Bacon (center panel; accumulation mean shape: 50 and 1.5, respectively; memory mean and strength: 0.5 and 10, respectively). Both produce similar median modeled ages, but Undatable produces wider uncertainty (right panel) near sedimentation rate inflections that are characterized by scatter in age-depth determinations (shaded region).

increases uncertainty at sediment rate inflection points because the depth of the change in rate is dependent on the depth and number of age determinations.

Thus, we find the uncertainty produced by Undatable to be more appropriate to our setting, because it incorporates uncertainty due to both age-depth reversals as well as inflections in sedimentation rate. Figure 3 shows Bacon and Undatable age models run with parameters producing very similar median modeled ages. The primary difference is the increased uncertainty in the Undatable model near the large changes in sedimentation rate, which we believe is most appropriate given the nature of the data.

DISCUSSION

Rapid Changes of Sedimentation Rates Corresponding the MWPs

The variation of the sedimentation rate of core VER99G12, is characterized by striking increases at 19.5, 18.3, 13.5, 10.2, and 9.5 ka (Figure 4), which are corresponding to the age reversal layers (Table 1). Apparent age reversals were observed in these layers, corresponding to ca. 19, 14, and 11.5 ka. Such age reversals at the same periods (ca. 19 and 14 ka) have been reported in the sediment core from Qinghai Lake (Zhou et al. 2016). Zhou et al. (2016) pointed out that old organic radiocarbon inputs to the Qinghai Lake sediment core at ca. 19 and 14 cal kyr BP could be caused by significant inputs of the meltwater from the glaciers around Qinghai Lake.

These significant increases in the sedimentation rates at 18.3 and 13.5 ka in the core VER99G12 happen just after the remarkable climatic warming events associated with the millennia of deglacial global sea level rise of 120 m in maximum (Yokoyama and Esat 2011). These sea level rises were caused by the large volume meltwater input to the oceans at 19 ka (meltwater pulse; MWP-1A0; Yokoyama et al. 2000; Clark et al. 2004; Yokoyama and Esat 2011) and 14.2–13.7 ka (MWP-1A; Deschamps et al. 2012). On the other hand, the rapid change in the sedimentation rate at 9.5 ka in the core VER99G12 was ca. 2000 years younger than the MWP-1B at 11.5 ka (Bard et al. 2010; Figure 4). Since the sampling site of the core VER99G12 was faced to the Selenga River inflow (Figure 1B and 1C), the deposition materials in the core VER99G12 could be strongly influenced from the Selenga River input (Kuzumin et al. 2000). Since Lake Baikal has large lake watershed

https://doi.org/10.1017/RDC.2023.63 Published online by Cambridge University Press

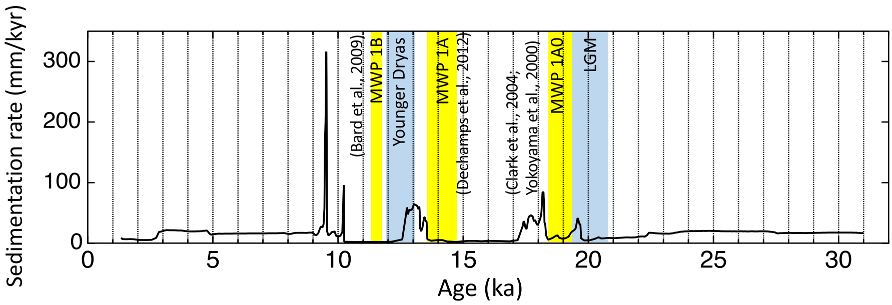

Figure 4 The profiles of sedimentation rate with calibrated age in the core VER99G12. The periods of global climate events for the Last Glacial Maximum, the MWP events and Younger Dryas event were highlighted in blue and yellow bars.

(Figure 1B) and the Selenga River inflow has ca. 50% of the total river input, the lake level has been mainly controlled by the Selenga River inflow and the evaporation at the warm and cold climate stage, respectively (Urabe et al. 2004; Osipov and Khlystov 2010). Seismic and geophysical analysis have revealed drastic lake-level changes repeatedly at the climate transition between the last glacial and the post-glacial period (Urabe et al. 2004; Nara et al. 2014). The lake level of Lake Baikal at MIS2 was estimated at 11–15 lower than present level (Urabe et al. 2004). However, the detection of pollen in core VER99G12 during MIS2 means that the Selenga River inflow did not cease (Shichi et al. 2013). Based on the pollen analysis (Shichi et al. 2013), tundra steppe vegetation was established in the Lake Baikal watershed around 18.5 ka during the first MWP period. This means that the vegetation in the Lake Baikal watershed at 18.5 ka was characterized by the expansion of permafrost and dominance of grassland. In contrast, during the second phase of rapid sedimentation at 13.5 ka witnessed the growth of aquatic vegetation such as spruce, alder and willow along streams in the Baikal Lake lowlands (Shichi et al. 2013) indicating a wet climate condition attributed to increased precipitation. Therefore, the rapid sedimentation rate at 13.5 ka was influenced not only by inflow water resulting from the permafrost thawing but also from precipitation in the Lake Baikal watershed.

During MIS2, the major inflow through the Selenga River to Lake Baikal was the melt water from the local glacier around the lake, although the precipitation was 25–50% lower than modern-day precipitation (Osipov and Khlystov 2010). Today, permafrost expands over the whole Lake Baikal watershed and thermokarst lakes have developed in the modern Lake Baikal watershed, indicating repeated permafrost thawing during the glacial period (Törnqvist et al. 2014). A recent study showed the dominance of icesheets in Scandinavia and North America as a source of meltwater during MWP-1A, rather than from those of the Antarctic (Lin et al. 2021). Also, significant increase in river water inflow to Qinghai Lake in China at the MWP events have been reported (Zhou et al. 2016). Our result suggested the observation for the change in the hydrological systems corresponding with the MWP events should be applicable to the lake with a significant melting glacier around the lake.

Re-Evaluating the Biological Activity in Lake Baikal for 31 ka with the Alternative Age-Depth Model

Based on the alternative age-depth model of core VER99G12 using *Undatable*, we reformed the age profiles of total organic carbon (TOC) and the mean grain size (MGS) from the core

https://doi.org/10.1017/RDC.2023.63 Published online by Cambridge University Press

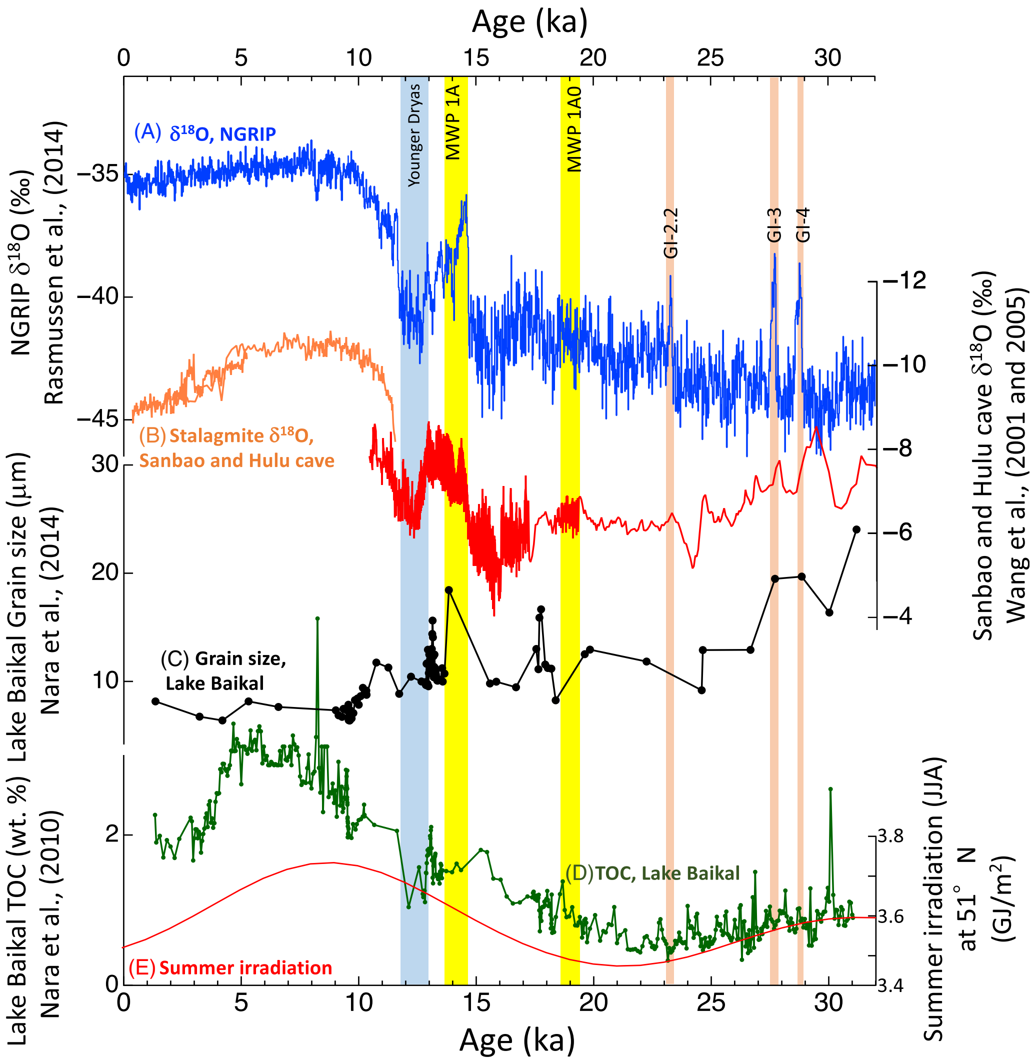

Figure 5 The comparison of the core VER99G12 records with other climate records. (A) $\delta^{18}O$ record from NGRIP ice core (blue; Rasmussen et al. 2014)); (B) $\delta^{18}O$ records from Sanbao and Hulu cave stalagmite (orange and red, respectively; Wang et al. 2005, 2001); (C) mean grain size and (D) TOC from the core VER99G12 in Lake Baikal (black and green, respectively, data from Nara et al. 2014); (E) July 51°N integrated irradiation for summer (JJA; day of year 152–243) (red; calculated following Lougheed (2022) using the orbital parameters of Laskar et al. (2004) and solar constant of 1361 Wm^{-2}).

VER99G12, which represent for the biological activity and the hydrological change, respectively (Figure 5; Nara et al. 2014). Biological activity in Lake Baikal for the last 32 ka inferred from TOC variations showed the synchronous variation with the summer isolation at 51°N on the whole (Figure 5). But also, the TOC profile of VER99G12 has small fluctuations as superimposed variations. Corresponding with the periods of increase in the sedimentation rates at 18.0 and 13.5 ka, the positive peaks of TOC concentration are also observed (Figure 5D). As well as TOC variation, despite of the sparse profile, the MGS variation from the Lake Baikal sediment core shows temporal increases at the above periods, which result from the high flux of the Selenga River input into the Lake Baikal (Figure 5C). The significant inflow of the Selenga River into the lake brings a significant nutrient load into the lake, resulting in the large biological activity in Lake Baikal (Nara et al. 2014). As well as warm periods, the temporal decreases in TOC of the core were observed at the LGM and YD (Figure 5). Therefore, the variations of biological activity and the grain size agree with the significant input of the Selenga River water into the lake at after the MWPs. These results mean that the alternative ^{14}C age calculated by IntCal20 with the *Undatable* age model for the core VER99G12 can be used to exploit the new findings of the environmental and biological changes in the Eurasian continental area inferred from the lake sediment core corresponding with the global climate changes.

SUMMARY

The rapid changes in the sedimentation rate corresponding with the global climate events, such as the MWPs, are observed from the Lake Baikal sediment core. The striking increase in the sedimentation rate were recorded at 18.3 and 13.5 ka, which are just after the periods of the MWP events. The signal of the melting glacier around the lake at 18.3 and 13.5 ka manifested as these rapid increases in the sedimentation rates. These sedimentation rate changes at 18.3 and 13.5 ka from the core VER99G12 were distinct variations comparing with other sediment cores from the Academician Ridge in Lake Baikal. The topographical feature of the Buguldeika Saddle, which is the sampling site of this study, manifested the change of inflow volume of Selenga River into the lake. The concurrent increases in TOC and the MGS at the 18.3 and 13.5 ka also support our interpretation that the high load of the nutrient for the biological activity to the lake caused by the high input of the river water at these periods.

ACKNOWLEDGMENTS

Editor-in-Chief A. J. T. Jull, Associate Editor Y. Kuzmin, and three anonymous reviewers are acknowledged for their helpful comments on the work, which helped to improve our manuscript. We would like to express our gratitude to Dr. Yunus Baykal for his help in constructing the age model using Bacon. The authors thank the staff of the TONO geoscience center, JAEA, for the sample preparation and ^{14}C measurements. Special thanks to Dr. Takayuki Omori at Tokyo University and the member of the Chronological Research Group at the Institute for Space–Earth Environmental Research in Nagoya University for their valuable suggestions and comments. We also gratefully acknowledge the Russian and Japanese participants for collecting the VER99G12 sediment core in the summer of 1999. This study was partly supported by JSPS KAKENHI Grant-in-Aid for Young Scientists (B) Grant Number 2674002, and for (C) Grant Number 22K12356 and for F.N.

REFERENCES

Antipin V, Afonina T, Badalov O, Bezrukova E, Bukharov A, Bychinsky V, Dmitriev AA, Dorofeeva R, Duchkov A, Esipko O, et al. 2001. The new bdp-98 600-m drill core from Lake Baikal: a key Late Cenozoic sedimentary section in continental Asia. Quaternary International 80–81:19–36.

Arzhannikov SG, Ivanov AV, Arzhannikova AV, Demonterova EI, Jansen JD, Preusser F, Kamenetsky VS, Kamenetsky MB. 2018. Catastrophic events in the quaternary outflow history of Lake Baikal. Earth-Science Reviews 177:76–113.

Bard E, Hamelin B, Delanghe-Sabatier D. 2010. Deglacial meltwater pulse 1b and younger dryas sea levels revisited with boreholes at Tahiti. Science 327(5970):1235–1237.

Blaauw M, Christen JA. 2011. Flexible paleoclimate age-depth models using an autoregressive gamma process. Bayesian Analysis 6(3):457–474.

Chebykin EP, Goldberg EL, Kulikova NS, Zhuchenko NA, Stepanova OG, Malopevnaya

YA. 2007. A method for determination of the isotopic composition of authigenic uranium in baikal bottom sediments. Russian Geology and Geophysics 48(6):468–477.
Clark PU, McCabe AM, Mix AC, Weaver AJ. 2004. Rapid rise of sea level 19,000 years ago and its global implications. Science 304(5674):1141–1144.
Colman SM, Jones GA, Rubin M, King JW, Peck JA, Orem WH. 1996. AMS radiocarbon analyses from Lake Baikal, Siberia: challenges of dating sediments from a large, oligotrophic lake. Quaternary Science Reviews 15(7):669–684.
Colman SM, Peck JA, Karabanov EB, Carter SJ, Bradbury JP, King JW, Williams DF. 1995. Continental climate response to orbital forcing from biogenic silica records in Lake Baikal. Nature 378(6559):769–771.
Demory F, Nowaczyk NR, Witt A, Oberhänsli H. 2005. High-resolution magnetostratigraphy of Late Quaternary sediments from Lake Baikal, Siberia: timing of intracontinental paleoclimatic responses. Global and Planetary Change 46(1):167–186.
Deschamps P, Durand N, Bard E, Hamelin B, Camoin G, Thomas AL, Henderson GM, Okuno J, Yokoyama Y. 2012. Ice-sheet collapse and sea-level rise at the bolling warming 14,600 years ago. Nature 483(7391):559–564.
Horiuchi K, Matsuzaki H, Kobayashi K, Goldberg EL, Shibata Y. 2003. 10Be record and magnetostratigraphy of a miocene section from Lake Baikal: re-examination of the age model and its implication for climatic changes in continental Asia. Geophysical Research Letters 30(12).
Horiuchi K, Minoura K, Hoshino K, Oda T, Nakamura T, Kawai T. 2000. Palaeoenvironmental history of Lake Baikal during the last 23000 years. Palaeogeography Palaeoclimatology Palaeoecology 157(1–2):95–108.
Ishiwa T, Yokoyama Y, Miyairi Y, Obrochta S, Sasaki T, Kitamura A, Suzuki A, Ikehara M, Ikehara K, Kimoto K, et al. 2016. Reappraisal of sea-level lowstand during the Last Glacial Maximum observed in the Bonaparte Gulf sediments, northwestern Australia. Quaternary International 397:373–379.
Karabanov E, Williams D, Kuzmin M, Sideleva V, Khursevich G, Prokopenko A, Solotchina E, Tkachenko L, Fedenya S, Kerber E, et al. 2004. Ecological collapse of Lake Baikal and lake hovsgol ecosystems during the last glacial and consequences for aquatic species diversity. Palaeogeography Palaeoclimatology Palaeoecology 209(1–4):227–243.
Kashiwaya K, Ochiai S, Sakai H, Kawai T. 2001. Orbit-related long-term climate cycles revealed in a 12-myr continental record from Lake Baikal. Nature 410(6824):71–74.
Katsuta N, Ikeda H, Shibata K, Saito-Kokubu Y, Murakami T, Tani Y, Takano M, Nakamura T, Tanaka A, Naito S, et al. 2018. Hydrological and climate changes in southeast siberia over the last 33 kyr. Global Planet Change 164:11–26.
Kuzumin MI, Williams DF, Kawai T. 2000. Lake Baikal: a mirror in time and space for understanding global change processes. Tokyo: Elsevier.
Laskar J, Robutel P, Joutel F, Gastineau M, Correia ACM, Levrard B. 2004. A long-term numerical solution for the insolation quantities of the Earth. Astronomy & Astrophysics 428:261–285.
Lin Y, Hibbert FD, Whitehouse PL, Woodroffe SA, Purcell A, Shennan I, Bradley SL. 2021. A reconciled solution of meltwater Pulse 1a sources using sea-level fingerprinting. Nature Communications 12(1):2015.
Lougheed BC. 2022. Orbital, the Box – an Interactive Educational Tool for In-depth Understanding of Astronomical Climate Forcing. Open Quaternary. 8, 10. https://doi.org/10.5334/oq.100
Lougheed, BC, Obrochta, SP. 2016. MatCal: open source Bayesian ^{14}C age calibration in MATLAB. Journal of Open Research Software. 4, e42. https://doi.org/10.5334/jors.130
Lougheed BC, Obrochta SP. 2019. A rapid, deterministic age-depth modeling routine for geological sequences with inherent depth uncertainty. Paleoceanography and Paleoclimatology 34(1):122–133.
Nara FW, Watanabe T, Kakegawa T, Minoura K, Imai A, Fagel N, Horiuchi K, Nakamura T, Kawai T. 2014. Biological nitrate utilization in south Siberian lakes (Baikal and Hovsgol) during the last glacial period: The influence of climate change on primary productivity. Quaternary Science Reviews 90:69–79.
Nara FW, Watanabe T, Nakamura T, Kakegawa T, Katamura F, Shichi K, Takahara H, Imai A, Kawai T. 2010. Radiocarbon and stable carbon isotope ratio data from a 4.7-m-long sediment core of Lake Baikal (southern Siberia, Russia). Radiocarbon 52(3):1449–1457.
Obrochta S, Andrén T, Fazekas S, Lougheed BC, Snowball I, Yokoyama Y, Miyairi Y, Kondo R, Kotilainen A, Hyttinen O. 2017. The undatables: quantifying uncertainty in a highly expanded Late Glacial—Holocene sediment sequence recovered from the deepest Baltic Sea basin—IODP Site M0063. Geochemistry, Geophysics, Geosystems 18:858–871.
Obrochta SP, Yokoyama Y, Yoshimoto M, Yamamoto S, Miyairi Y, Nagano G, Nakamura A, Tsunematsu K, Lamair L, Hubert-Ferrari A, et al. 2018. Mt. Fuji Holocene eruption history reconstructed from proximal lake sediments and high-density radiocarbon dating. Quaternary Science Reviews 200:395–405.
Ochiai S, Kashiwaya K. 2003. Hydro-geomorphological changes and sedimentation processes printed in sediments from Lake Baikal. Long continental records from Lake Baikal. Springer Japan. p. 297–312.

https://doi.org/10.1017/RDC.2023.63 Published online by Cambridge University Press

Ochiai S, Kashiwaya K. 2005. Climato-hydrological environment inferred from Lake Baikal sediments based on an automatic orbitally tuned age model. Journal of Paleolimnology 33(3):303–311.
Osipov EY, Khlystov OM. 2010. Glaciers and meltwater flux to Lake Baikal during the last glacial maximum. Palaeogeography Palaeoclimatology Palaeoecology 294(1–2):4–15.
Prokopenko AA, Hinnov LA, Williams DF, Kuzmin MI. 2006. Orbital forcing of continental climate during the pleistocene: A complete astronomically tuned climatic record from Lake Baikal, se siberia. Quaternary Science Reviews 25(23–24):3431–3457.
Prokopenko AA, Karabanov EB, Williams DF, Kuzmin MI, Khursevich GK, Gvozdkov AA. 2001. The detailed record of climatic events during the past 75,000yrs BP from the Lake Baikal drill core bdp-93-2. Quaternary International 80–81:59–68.
Rasmussen SO, Bigler M, Blockley SP, Blunier T, Buchardt SL, Clausen HB, Cvijanovic I, Dahl-Jensen D, Johnsen SJ, Fischer H, et al. 2014. A stratigraphic framework for abrupt climatic changes during the last glacial period based on three synchronized greenland ice-core records: refining and extending the intimate event stratigraphy. Quaternary Science Reviews 106:14–28.
Reimer PJ, Austin WEN, Bard E, Bayliss A, Blackwell PG, Bronk Ramsey C, Butzin M, Cheng H, Edwards RL, Friedrich M, et al. 2020. The IntCal20 Northern Hemisphere radiocarbon age calibration curve (0–55 cal kyr BP). Radiocarbon 62(4):725–757.
Shichi K, Kawamuro K, Takahara H, Hase Y, Maki T, Miyoshi N. 2007. Climate and vegetation changes around Lake Baikal during the last 350,000 years. Palaeogeography Palaeoclimatology Palaeoecology 248(3–4):357–375.
Shichi K, Takahara H, Hase Y, Watanabe T, Nara FW, Nakamura T, Tani Y, Kawai T. 2013. Vegetation response in the southern Lake Baikal region to abrupt climate events over the past 33calkyr. Palaeogeography, Palaeoclimatology, Palaeoecology 375(Supplement C):70–82.
Shimaraev MN, Granin NG, Zhdanov AA. 1993. Deep ventilation of Lake Baikal waters due to spring thermal bars. Limnology and Oceanography 38(5):1068–1072.
Soma Y, Tani Y, Soma M, Mitake H, Kurihara R, Hashomoto S, Watanabe T, Nakamura T. 2006. Sedimentary steryl chlorin esters (sces) and other photosynthetic pigments as indicators of paleolimnological change over the last 28,000 years from the Buguldeika saddle of Lake Baikal. Journal of Paleolimnology 37(2):163–175.
Swann GEA, Mackay AW, Vologina E, Jones MD, Panizzo VN, Leng MJ, Sloane HJ, Snelling AM, Sturm M. 2018. Lake Baikal isotope records of holocene central asian precipitation. Quaternary Science Reviews 189:210–222.
Tani Y, Nara F, Soma Y, Soma M, Itoh N, Matsumoto GI, Tanaka A, Kawai T. 2009. Phytoplankton assemblage in the plio-pleistocene record of Lake Baikal as indicated by sedimentary steryl chlorin esters. Quaternary International 205(1):126–136.
Törnqvist R, Jarsjö J, Pietroń J, Bring A, Rogberg P, Asokan SM, Destouni G. 2014. Evolution of the hydro-climate system in the Lake Baikal basin. Journal of Hydrology 519:1953–1962.
Urabe A, Tateishi M, Inouchi Y, Matsuoka H, Inoue T, Dmytriev A, Khlystov OM. 2004. Lake-level changes during the past 100,000 years at Lake Baikal, southern Siberia. Quaternary Research 62(2):214–222.
Waelbroeck C, Lougheed BC, Vazquez Riveiros N, Missiaen L, Pedro J, Dokken T, Hajdas I, Wacker L, Abbott P, Dumoulin J-P, et al. 2019. Consistently dated atlantic sediment cores over the last 40 thousand years. Scientific Data 6(1):165.
Wang Y, Cheng H, Edwards RL, He Y, Kong X, An Z, Wu J, Kelly MJ, Dykoski CA, Li X. 2005. The holocene asian monsoon: links to solar changes and North Atlantic climate. Science 308(5723): 854–857.
Wang YJ, Cheng H, Edwards RL, An ZS, Wu JY, Shen CC, Dorale JA. 2001. A high-resolution absolute-dated late pleistocene monsoon record from hulu cave, china. Science 294(5550):2345–2348.
Watanabe T, Nakamura T, Kawai T. 2007. Radiocarbon dating of sediments from large continental lakes (Lakes Baikal, Hovsgol and Erhel). Nuclear Instruments and Methods in Physics Research Section B: Beam Interactions with Materials and Atoms 259(1):565–570.
Watanabe T, Nakamura T, Nara FW, Kakegawa T, Nishimura M, Shimokawara M, Matsunaka T, Senda R, Kawai T. 2009a. A new age model for the sediment cores from academician ridge (Lake Baikal) based on high-time-resolution AMS ^{14}C data sets over the last 30 kyr: paleoclimatic and environmental implications. Earth and Planetary Science Letters 286(3–4):347–354.
Watanabe T, Nakamura T, Watanabe Nara F, Kakegawa T, Horiuchi K, Senda R, Oda T, Nishimura M, Inoue Matsumoto G, Kawai T. 2009b. High-time resolution AMS ^{14}C data sets for Lake Baikal and Lake Hovsgol sediment cores: changes in radiocarbon age and sedimentation rates during the transition from the last glacial to the Holocene. Quaternary International 205:12–20.
Webster JM, Braga JC, Humblet M, Potts DC, Iryu Y, Yokoyama Y, Fujita K, Bourillot R, Esat TM, Fallon S, et al. 2018. Response of the Great Barrier Reef to sea-level and environmental changes over the past 30,000 years. Nature Geoscience 11:426–432.

Yokoyama Y, Esat TM. 2011. Global climate and sea level enduring variability and rapid fluctuations over the past 150,000 years. Oceanography 24(2):54–69.

Yokoyama Y, Lambeck K, De Deckker P, Johnston P, Fifield LK. 2000. Timing of the last glacial maximum from observed sea-level minima. Nature 406(6797):713–716.

Zhou W, Liu T, Wang H, An Z, Cheng P, Zhu Y, Burr GS. 2016. Geological record of meltwater events at qinghai lake, china from the past 40 ka. Quaternary Science Reviews 149:279–287.